

Real-time Contact State Estimation in Shape Control of Deformable Linear Objects under Small Environmental Constraints

Kejia Chen^{1*}, Zhenshan Bing^{1*}, Fan Wu^{1*}, Yansong Wu¹, Liding Zhang¹, Sami Haddadin¹, Alois Knoll¹

Abstract—Controlling the shape of deformable linear objects using robots and constraints provided by environmental fixtures has diverse industrial applications. In order to establish robust contacts with these fixtures, accurate estimation of the contact state is essential for preventing and rectifying potential anomalies. However, this task is challenging due to the small sizes of fixtures, the requirement for real-time performances, and the infinite degrees of freedom of the deformable linear objects. In this paper, we propose a real-time approach for estimating both contact establishment and subsequent changes by leveraging the dependency between the applied and detected contact force on the deformable linear objects. We seamlessly integrate this method into the robot control loop and achieve an adaptive shape control framework which avoids, detects and corrects anomalies automatically. Real-world experiments validate the robustness and effectiveness of our contact estimation approach across various scenarios, significantly increasing the success rate of shape control processes.

I. INTRODUCTION

Controlling the shape of deformable linear objects (DLOs) with robot manipulators has a wide range of industrial applications, such as cable routing [1], wire-harness assembly in manufacturing [2], or manipulation of endoscopes in robotic surgeries [3]. To provide additional constraints on DLOs, contacts from environmental fixtures are often utilized in these processes [1], [4]–[8]. Reliable contact state estimation between fixtures and DLOs is crucial for prevention of potential anomalies such as misalignment or insufficient pushing, and for enhancing the overall robustness of the shape control system. One typical fixture which has been widely used in manufacturing is clip-like fixtures. Due to their own deformations, clip-like fixtures introduce a dynamic and multi-stage contact process (see Fig 1): as the DLO advances towards the clip, it initially makes contact with the clip’s opening. Subsequently, as the DLO is pushed inward, the clip is forced to open to let the object in. Once the object is securely fastened inside the clip, the contact is detached, unless the object moves further and collides with the rear part of the clip.

Existing contact estimation approaches typically rely on visual perception or robot motion information [9]–[11]. However, they are not reliable to be applied to contacts in clip fixing scenarios. Firstly, the small size of fixtures and the resulting limited displacements of robots during clip fixing leads to requirements for precise segmentation as well as strict real-time responses. As a result, visual perception

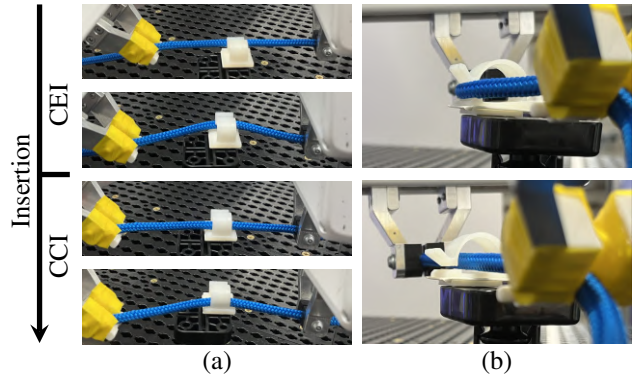


Fig. 1: Clip fixing and DLO deformation. (a) Top views. From top to bottom: contact-insertion-fixed-overforce movement. (b) Left views. Top: insertion; bottom: fixed.

algorithms used in prior works [4]–[6] are not practical due to their dependence on slower image processing. Secondly, the contact is established not with the robot but with the DLO itself, which makes direct contact measurement impossible [4]. In the case of a DLO, its contact state lags behind the robot motion due to the deformation. For example, in Fig 1(a), despite that we have stretched the grasped DLO to be tense, noticeable deformation still exists, and the two robots may continue advancing even when DLO is still blocked.

Inspired by the pivotal role of tactile information in human perception of deformable objects, we present a real-time method based on contact forces that can accurately estimate contact state of DLOs subject to various environmental constraints. We then integrate the contact state estimation method into the DLO shape control framework of two robotic manipulators, which dynamically adjusts its parameters in case of anomalies.

II. METHODOLOGY

A. Clip Fixing Process

We formulate the clip fixing process based on the clip-fixing skill introduced in our prior work [1]. As is shown in Fig 2, the movement of robots as well as the cable is described in an object-centered coordinate frame. The clip fixing process is defined as a directed transition graph of manipulation primitives (MPs). In contrast to [1], we redefine every MP to consist solely of a desired feedforward force \mathbf{f} controlled under an adaptive impedance controller [12], without controlling linear velocity $\dot{\mathbf{x}}^d$. Initially, both robots securely grasp each end of a DLO segment. As two robot exert forces $\mathbf{f}_{\text{stretch}} = [\pm f_{\text{stretch}}, 0, 0]^T$ in the opposite direction, the segment is stretched until it becomes tense (Fig.2(a)). $\mathbf{f}_{\text{stretch}}$ is maintained throughout the subsequent stages. Following this, robots guide the segment with a pushing force $\mathbf{f}_{\text{push}} = [0, f_{\text{push}}, 0]^T$ to establish contact with the

¹ School of Computation, Information and Technology, Technical University of Munich, Germany. kejia.chen@tum.de

* Equal contribution.

The authors acknowledge the financial support by the Bavarian State Ministry for Economic Affairs, Regional Development and Energy (StMWi) for the Lighthouse Initiative KLFABRIK (Phase I: Infrastructure as well as the research and development program under grant no. DIK0249). Please note that S. Haddadin had a potential conflict of interest as a shareholder of Franka Emika GmbH.

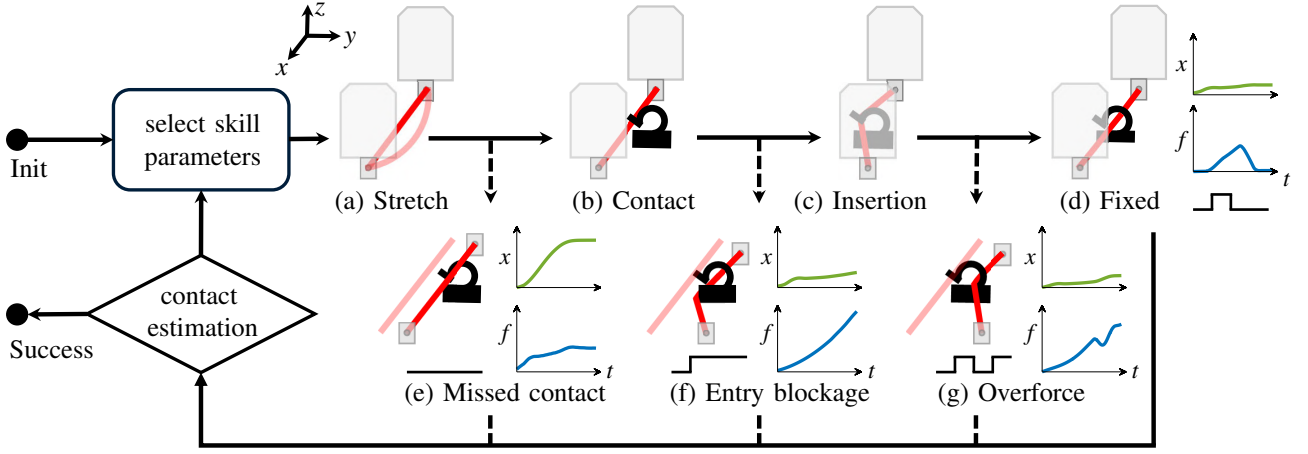


Fig. 2: Clip fixing process. The red curve represents the DLO. The black fixture represents the clip. The gray polygon represents the robot hand and finger tips. (a), (b), (c) and (d) in the first row describe the ideal clip fixing process. (e), (f), (g) in the second row describe the failures which may happen at different stages. The tendency of displacement (green curve) and contact force (blue curve) are depicted next to each failure. For simplicity, the hand is omitted in the second row.

clip (Fig.2(b)). Upon contact detection, instead of applying a constant pushing force, f_{push} rises gradually from zero: $f_{push}(0) = 0$ and $\frac{df_{push}(t)}{dt} > 0$ (Fig.2(c)). Once the DLO segment is fully inserted, the robots cease applying forces and further motion (Fig.2(d)).

Although experiments in [1] have substantiated the effectiveness of the clip-fixing skill above, there exists some issues which may diminish the framework’s robustness:

- **Missed contact** (Fig 2(e)). If the grasped DLO passes over the clip opening, no contact is established between the object and the clip. Consequently, the DLO continues to move forward alongside the clip.
- **Entry blockage** (Fig 2(f)). If the grasped DLO moves below the clip opening, it will be blocked by the fixture base. Contact is maintained once established until the skill exits.
- **Overforce movement** (Fig 2(g)). Excessive applied force f_{push} or a delay in force removal after insertion can cause the DLO to continue moving forward, eventually colliding with the clip’s rear end.

We notice that these anomalies happen at different stages of the clip fixing process with different contact patterns, and can be detected and avoided by accurate estimation of DLO’s current contact state with the clip.

B. Contact Estimation

In all MPs following stretching, the grasped DLO is stretched by $\mathbf{f}_{stretch}$ and at the same time pushed by \mathbf{f}_{push} into the clip. Once it establishes contact with the clip, it is also under contact force \mathbf{f}_c . The general dynamics of the DLO in y direction can be described as

$$m \cdot \ddot{x}(t) = f_{push} - f_c(t), \quad (1)$$

which can be conceptualized as a system that takes f_{push} as input and generates outputs in the form of \ddot{x} and f_c . We define a contact establishment indicator (CEI) and a contact change indicator (CCI) to estimate the initial contact establishment and following contact changes respectively by analyzing the interrelationship between the input and output.

1) **Contact Change Indicator (CCI)**: As shown in Fig 1(a), the insertion MP describes the process after the DLO has contacted the clip until it is inserted in and the contact terminates. Inspired by the definition of stiffness (ratio of the resulting deformation to the applied force), we define an indicator for describing the contact change in this process as the rate of change of the resulting contact force to the feedforward force:

$$\rho_c = \frac{df_c}{df_{push}}. \quad (2)$$

To establish a robust relationship between f_c and f_{push} , we set two prerequisites for the insertion MP. Firstly, the grasped DLO is stretched to be tense and already in a solid contact with the clip. Thus, the deformation of DLO can be neglected, i.e., θ is almost a constant. In addition, after the contact MP, robots are forced to pause moving until the velocity is close to zero before the insertion MP starts. These prerequisites ensure that at each time point between establishing contact and being inserted into the clip, the DLO can be approximated as quasi-static and the acceleration could be neglected so that $\rho_c \approx 1$.

As $f_{push}(t)$ rises, an abrupt drop in ρ_c occurs at the moment when the DLO is inserted into the clip and the contact disappears. To capture this moment, we make prediction of ρ_c in the future: at each time point t , we consider $\rho_c(t)$ as a random variable following a Gaussian distribution

$$\rho_c(t) \sim \mathcal{N}(\mu_{t-1}, \sigma_{t-1}^2), \quad (3)$$

where μ_{t-1} and σ_{t-1} represent the cumulative average and standard deviation until time step $t-1$, respectively. When the contact remains stable, $\rho_c(t)$ should conform to our prediction. The instant of a contact change, whether a termination or a new establishment, is detected when $\rho_c(t)$ deviates from the prediction, i.e., when it falls outside a confidence interval (CI) specified by the Z-score. The condition for contact detachment is formulated as $\rho_c(t) < \mu_{t-1} - Z \cdot \sigma_{t-1}$. Similarly, the re-establishment condition is formulated as $\rho_c(t) > \mu_{t-1} + Z \cdot \sigma_{t-1}$.

2) **Contact Establishment Indicator (CEI)**: Given the first prerequisite of the insertion MP that θ should be quasi-static, we define an indicator for describing whether there is a solid

contact established between the clip and the DLO in the contact MP. This contact establishment indicator, denoted as ρ_e , is defined as the ratio of the contact force to the feedforward force:

$$\rho_e = \frac{f_c}{f_{push}}. \quad (4)$$

In theory, the moment when contact is established can be detected by simply measuring whether $f_c > 0$. In practice, however, the contact force detected by robots $f_c^{ext}(t)$ is usually non-zero as it includes additionally noise and especially measurement error arising from acceleration $f_c^{ext}(t) = f_c(t) + m_e \cdot \ddot{x}(t)$. Before any contact is established, the acceleration $\ddot{x}(t) = \frac{f_{push}}{m}$ is relatively high and the measurement error cannot be ignored. This leads to the modified form of (1):

$$(m + m_e) \cdot \ddot{x}(t) = f_{push} - f_c(t). \quad (5)$$

As the deformation of the clip grows, both $f_c(t)$ and CEI rises. The second-order differential system in (5) will eventually reach an equilibrium point where $f_c(t) = f_{push}$ and $\rho_e = 1$, which marks the moment when θ becomes stable and a solid contact is established. In practice, we formulate the contact establishment condition with a threshold E that $\rho_e > E$.

C. Enhanced Shape Control

Based on CEI and CCI, the ideal clip fixing process as well as anomalies introduced in subsection II-A can be characterized by the contact force profile, more specifically, as sequences of contact establishment and detachment $\zeta = \{0, 1\}^n$, where 0 represents non-contact states and 1 represents established contact. The ideal clip fixing process is profiled as $\zeta^* = [0, 1, 0]$. The contact state sequences of each MP and anomaly are depicted in Fig 2.

We then combine the improved clip fixing skill with the shape tracking skill developed in our prior work [1] to form an enhanced adaptive shape control framework which could detect and correct anomalies automatically based on feedback provided by contact sequences. Arriving at one fixture ψ_i , the clip fixing skill starts and runs in iterations. In the first iteration, MP parameters are sampled randomly from respective uniform distributions. After each iteration, in case when anomalies are detected, the upper and lower ranges of the parameter distributions are updated respectively based on the difference between ζ_i and ζ^* , and MP parameters are sampled again from the updated distribution. This process is repeated until ζ^* is detected.

III. EXPERIMENTS

To evaluate the accuracy of the proposed contact estimation approach, we use two 7 DOF Franka Emika Panda robots for real-world experiments, both of which are equipped with joint torque sensors and provide 6-axis force torque estimation at the end-effectors. Throughout this process, all the fixtures remain anchored to the desk, maintaining constant poses.

A. Evaluation of Contact Change Detection

We evaluate the performance of CCI in comparison to two other intuitive indicators for contact change detection, namely, a constant contact threshold F_c and the contact force change rate df_c/dt , across various setups.

Across different rising Firstly, we compare performances under three different growing patterns of $f_{push}(t)$, each

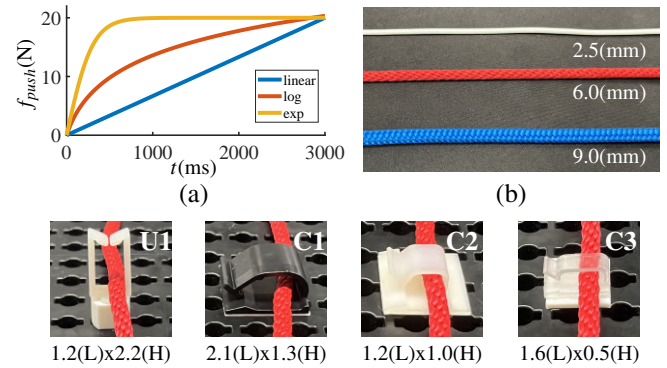


Fig. 3: Various settings for comparing contact change detection. (a) Different growing patterns of the $f_{push}(t)$. (b) Cables with different radius. (c) Various clip fixtures and sizes (Length x Height (cm)).

approximating a linear function, a logarithm function and an exponential function, as shown in Fig 3(a). We collect contact data by performing overforce movement with every growing pattern in Fig 3(a) at three different fixture poses P1, P2, and P3, with each setting repeated for 10 times. The number of successful contact change detection using each indicator is summarized in Table I. Overall, ρ_c achieves equal or higher success rate across different rising patterns.

TABLE I: Contact change detection accuracy I.

	F_c			df_c/dt			ρ_c (ours)		
	P1	P2	P3	P1	P2	P3	P1	P2	P3
linear	10	10	9	10	10	9	10	10	9
log	10	10	9	10	10	5	10	10	9
exp	10	1	4	9	1	2	10	10	5
success	1.0	0.7	0.73	0.96	0.7	0.53	1.0	1.0	0.83

Across different cables and clips Furthermore, we compare their performance on cables with different radius (Fig 3(b)) and clips of different sizes and opening directions (Fig 3(c)). The number of successful contact change detection using each indicator is listed in Table II. As the radius becomes smaller and the contact change turns less obvious, e.g. in the case of cable S with clip C1, ρ_c preserves the most robust performance.

TABLE II: Contact change detection accuracy II.

	F_c			df_c/dt			ρ_c (ours)		
	C1	C2	U1	C1	C2	U1	C1	C2	U1
L	10	0	10	10	10	10	10	10	10
M	10	0	10	10	10	10	10	10	10
S	4	0	0	4	0	0	10	10	0
success	0.48			0.71			0.88		

Finally, we evaluate the improvements our contact estimation approach brings to the shape control framework by comparing the success rate with and without contact estimation integrated. Four fixtures of three different types are mounted securely on the harness board. Each fixture is designed to have a slightly different offset δ_z in its z axis. These offsets are hard to be detected by visual observations but may lead to an anomaly in clip fixing. The results of clip fixing at each fixture are listed in Table III. For the complete shape control process, please refer to the video at <https://youtu.be/Ph9GsCaEKEg>.

TABLE III: Shape control experiments

	U1 ($\delta_z = -10\text{mm}$)	C1 ($\delta_z = 3\text{mm}$)	C3 ($\delta_z = 5\text{mm}$)	C3 ($\delta_z = 0\text{mm}$)
With	Success	Success	Success	Success
Without	Missed Contact	Entry Blockage	Entry Blockage	Success

REFERENCES

- [1] K. Chen, Z. Bing, F. Wu, Y. Meng, A. Kraft, S. Haddadin, and A. Knoll, "Contact-aware shaping and maintenance of deformable linear objects with fixtures," in *2023 IEEE/RSJ International Conference on Intelligent Robots and Systems (IROS)*, 2023, pp. 1–8.
- [2] G. E. Navas-Reascos, D. Romero, J. Stahre, and A. Caballero-Ruiz, "Wire harness assembly process supported by collaborative robots: Literature review and call for r&d," *Robotics*, vol. 11, no. 3, p. 65, 2022.
- [3] N. Haouchine, W. Kuang, S. Cotin, and M. Yip, "Vision-based force feedback estimation for robot-assisted surgery using instrument-constrained biomechanical three-dimensional maps," *IEEE Robotics and Automation Letters*, vol. 3, no. 3, pp. 2160–2165, 2018.
- [4] J. Zhu, B. Navarro, R. Passama, P. Fraise, A. Crosnier, and A. Cherubini, "Robotic manipulation planning for shaping deformable linear objects with environmental contacts," *IEEE Robotics and Automation Letters*, vol. 5, no. 1, pp. 16–23, 2019.
- [5] S. Huo, A. Duan, C. Li, P. Zhou, W. Ma, H. Wang, and D. Navarro-Alarcon, "Keypoint-based planar bimanual shaping of deformable linear objects under environmental constraints with hierarchical action framework," *IEEE Robotics and Automation Letters*, vol. 7, no. 2, pp. 5222–5229, 2022.
- [6] S. Jin, W. Lian, C. Wang, M. Tomizuka, and S. Schaal, "Robotic cable routing with spatial representation," *IEEE Robotics and Automation Letters*, vol. 7, no. 2, pp. 5687–5694, 2022.
- [7] G. A. Waltersson, R. Laezza, and Y. Karayiannidis, "Planning and control for cable-routing with dual-arm robot," in *2022 International Conference on Robotics and Automation (ICRA)*. IEEE, 2022, pp. 1046–1052.
- [8] F. Süberkrüb, R. Laezza, and Y. Karayiannidis, "Feel the tension: Manipulation of deformable linear objects in environments with fixtures using force information," in *2022 IEEE/RSJ International Conference on Intelligent Robots and Systems (IROS)*. IEEE, 2022, pp. 11 216–11 222.
- [9] Z. Erickson, A. Clegg, W. Yu, G. Turk, C. K. Liu, and C. C. Kemp, "What does the person feel? learning to infer applied forces during robot-assisted dressing," in *2017 IEEE International Conference on Robotics and Automation (ICRA)*. IEEE, 2017, pp. 6058–6065.
- [10] Y. Wang, D. Held, and Z. Erickson, "Visual haptic reasoning: Estimating contact forces by observing deformable object interactions," *IEEE Robotics and Automation Letters*, vol. 7, no. 4, pp. 11 426–11 433, 2022.
- [11] Y. Wi, P. Florence, A. Zeng, and N. Fazeli, "Virido: Visio-tactile implicit representations of deformable objects," in *2022 International Conference on Robotics and Automation (ICRA)*. IEEE, 2022, pp. 3583–3590.
- [12] L. Johannsmeier, M. Gerchow, and S. Haddadin, "A framework for robot manipulation: Skill formalism, meta learning and adaptive control," in *2019 International Conference on Robotics and Automation (ICRA)*. IEEE, 2019, pp. 5844–5850.